

Supplementary Information

Unveiling the solar-driven synergetic production of a cyclic fuel-additive and carbon-free solar fuel from biogenic furfural: mediated by a metal-free organic semiconductor

Shivali Dhingra, ^[a] Arpna Jaryal, ^[a] Deepak Kumar Chauhan, ^[a] and Kamalakannan Kailasam ^{*[a]}

[a] Advanced Functional Nanomaterials group, Institute of Nano Science and Technology (INST), Knowledge City, Sector 81, SAS Nagar, Manauli PO, Mohali, 140306, Punjab, India.

Corresponding Author: Kamalakannan Kailasam

*E-mail: kamal@inst.ac.in, kkamal17@gmail.com

1. Experimental section

1.1. Materials

Urea, melamine, hydroxymethylfurfural (HMF), and methanol were bought from Sigma Aldrich. Ethylene glycol, furfural, and 2,5-diformylfuran were brought from TCI. Ethanol was brought from Changshu Hongsheng Fine Chemicals. All the chemicals were used without further purification.

1.2. Synthesis of UCN

5 g urea was weighed, placed in an alumina crucible, and calcined at 550 °C for 2 h in a Nabertherm furnace with a ramp rate of 5 °C min⁻¹. It was denoted by UCN throughout the manuscript.

1.3. Synthesis of MCN

5 g melamine was weighed and placed in an alumina crucible and calcined in N₂ flow at 550 °C for 2 h with the ramp rate of 5 °C min⁻¹. It was denoted by MCN throughout the manuscript.

1.4. Analytical techniques

The diffraction pattern of material was measured by PXRD (Powder X-ray diffraction) using Bruker D8 Advance diffractometer equipped with a scintillation counter detector, with Cu-K α radiation ($\lambda = 0.15418$ nm) source operating at 40 kV and 40 mA. UV-Visible

spectrophotometer (Agilent Cary 100) was used to measure the diffuse reflectance spectra of the solid sample, by using a reference as barium sulfate. The Brauner-Emmett-Teller (BET) and Barrett-Joyner-Halenda (BJH) method on the Autosorb iQ3 instrument (Quantachrome) was utilized to measure the specific surface area of the material using the isotherm obtained from physisorption measurements. X-ray photoelectron spectroscopy (XPS) was utilized to determine the elemental composition of the material by using Al K α X-ray source and an ultra-high vacuum monochromator. Transmission electron microscope (TEM) measurements were performed using JEOL at an operational voltage of 200 kV. The morphology of synthesized UCN was analyzed using JEOL field emission scanning electron microscopy (FESEM). *In-situ* Electron paramagnetic resonance (EPR) measurement was performed at room temperature using the Bruker A300-9.5/12/S/W instrument. Horiba Fluorolog instrument was employed to record the Solid-state Photoluminescence spectra (PL). After the photocatalytic reaction, the liquid product was analyzed by using a Shimadzu Gas Chromatography-Mass Spectrometer (GC-MS) fitted with a Stabilwax-MS column whereas the gaseous product (H₂) was estimated using Shimadzu Gas Chromatography with a thermal conductivity detector (TCD).

Electrochemical impedance spectroscopy (EIS)-Nyquist plot was carried out on Metrohm Autolab by using a standard three-electrode setup where Pt wire as counter electrode, Ag/AgCl (3 M KCl) as reference electrode, and glassy carbon electrode as working electrode. An aqueous solution of 0.2 M Na₂SO₄ was used as an electrolyte. The working electrode was prepared by coating slurry of UCN on a glassy carbon electrode having a diameter of 0.2 cm with subsequent overnight drying at room temperature. The Nyquist plot was recorded in the frequency range of 0.1 Hz - 20 kHz. UCN slurry was prepared by dispersing 10 mg of powder sample in 0.3 mL ethanol along with 15 μ L nafion solution under ultrasonication for 30 min.

Photo-electrochemical studies were carried out using Metrohm Autolab (M204 multichannel potentiostat galvanostat) with a three-electrode system, where Pt wire, Ag/AgCl (3.5 M KCl), and UCN-coated ITO (0.5 \times 0.5 cm) were used as counter, reference and working electrode, respectively. A 0.2 M aq. Na₂SO₄ solution was used as an electrolyte. The working electrode was prepared by coating a slurry of UCN on an Indium tin oxide (ITO) (0.5 \times 0.5 cm) electrode with subsequent overnight drying at room temperature. UCN slurry was prepared by dispersing 10 mg of a powder sample in 0.3 mL ethanol along with 15 μ L nafion solution under ultrasonication for 30 min. A Xenon lamp (400 W) with a cut-off filter of 420 nm was

used as a light source. EIS-Nyquist plot for UCN was recorded in the frequency range of 0.1 Hz to 10 kHz at the bias potential of 1.86 V vs reversible hydrogen electrode (RHE). Linear sweep voltammetry (LSV) curves were recorded with a scan rate of 50.0 mV s⁻¹. The Ag/AgCl electrode potential was converted to a RHE by using the following equation³

$$E(\text{RHE}) = E(\text{Ag/AgCl}) + 0.197 \text{ V} + \text{pH} \times 0.0592$$

1.5. Photocatalytic reaction procedure

The photocatalytic acetalization was carried out in a round bottom flask (RB) in the presence of visible light. In the reaction, a specific amount of UCN was mixed in 2 mL of the alcohol under sonication containing 0.1 mmol of the biomass-derived substrate. The solution was purged with O₂ gas and a balloon filled with oxygen gas was affixed to the flask. Photocatalytic Reaction was performed at room temperature under a 400 W xenon lamp with a 420 nm cut-off filter (Newport) (only allowed a visible spectrum of electromagnetic radiation). At regular intervals of time, the progress of the reaction was monitored. For recyclability, the photocatalyst was recovered by centrifuge, washed multiple times with water, and ethanol, and dried in a vacuum oven at 70 °C for 12 h before using it for the next cycle. The organic products were identified by using gas chromatography-mass spectrometry (GC-MS).

H₂O₂ was quantified by using the iodometry method. For this purpose, potassium hydrogen phthalate (KHP) of 0.1 M concentration and potassium iodide (KI) of 0.4 M concentration were freshly prepared. In 100 μL of the obtained reaction mixture, 450 μL of KI and 450 μL of KHP were added and placed in dark for 30 min. Under acidic conditions, H₂O₂ in the reaction mixture was reacted with iodine ion (I⁻) to produce triiodide ion (I₃⁻) which exhibits strong absorbance at 350 nm and can be detected by UV-Vis spectroscopy. Based on the calculated concentration of the triiodide ion (I₃⁻), the amount of H₂O₂ was quantified in the reaction mixture.

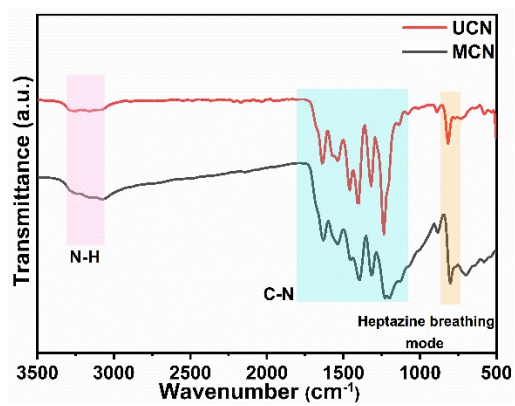


Figure S1. FTIR spectra of UCN and MCN.

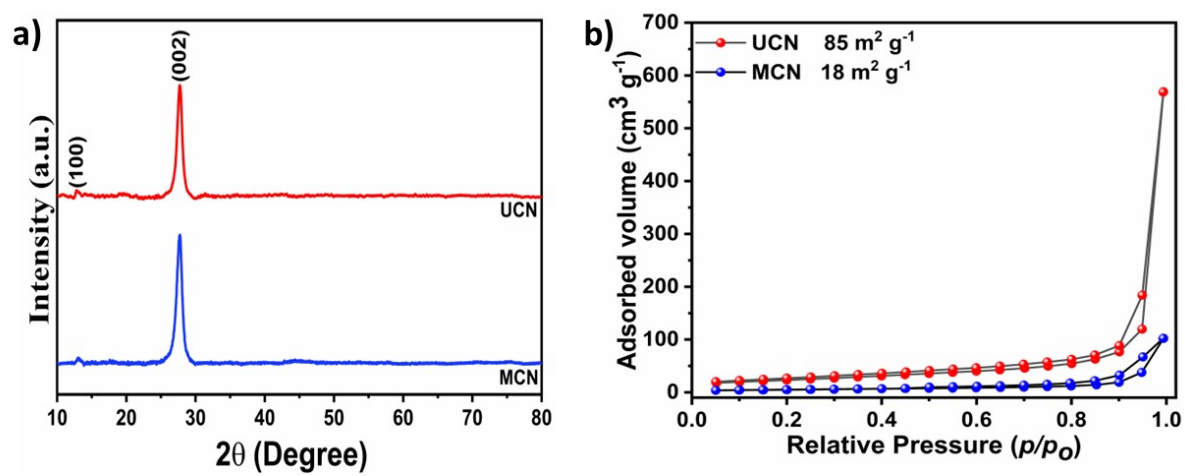


Figure S2. (a) XRD pattern of UCN and MCN; and (b) N₂ physisorption isotherms for UCN and MCN.

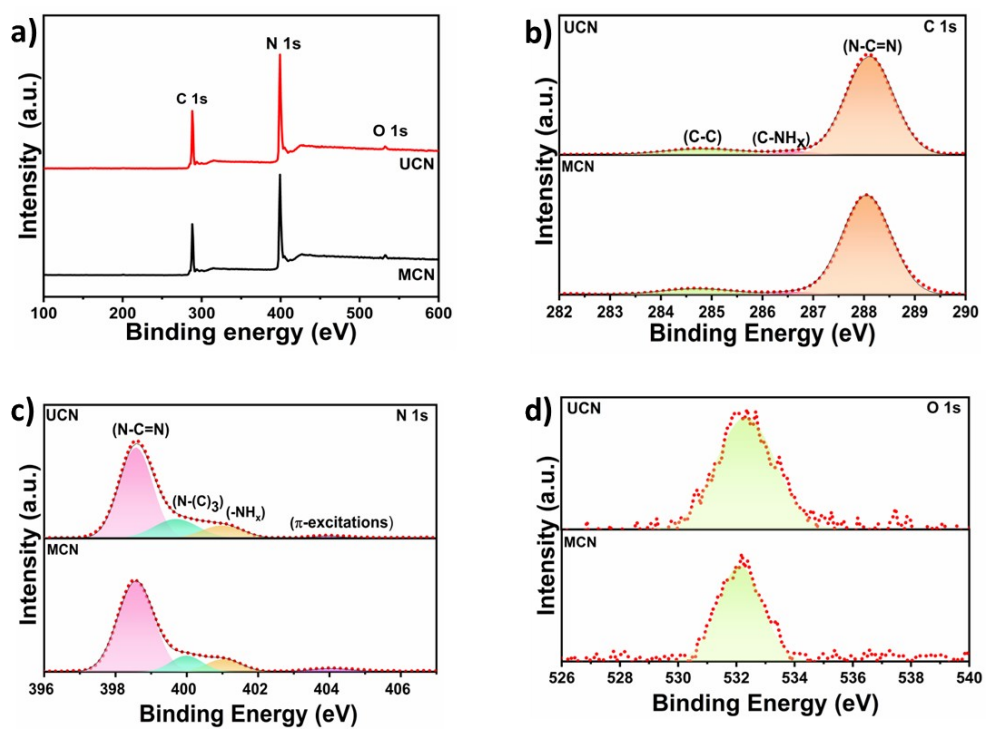


Figure S3. (a) XPS survey scan of UCN and MCN; and (b-d) XPS high-resolution spectra of C 1s, N 1s, and O 1s.

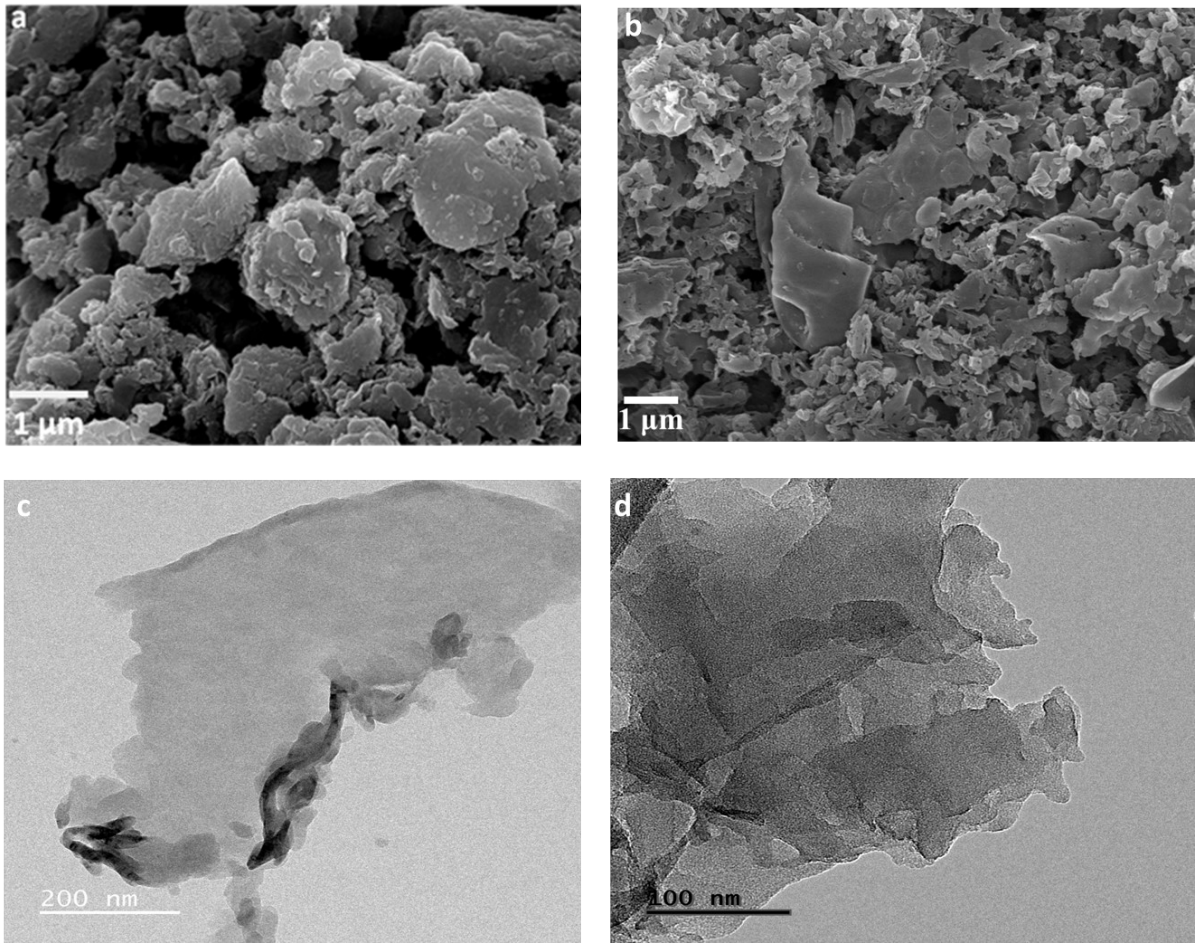


Figure S4. FE-SEM image of (a) UCN; (b) MCN; and TEM image of (a) UCN; (b) MCN.

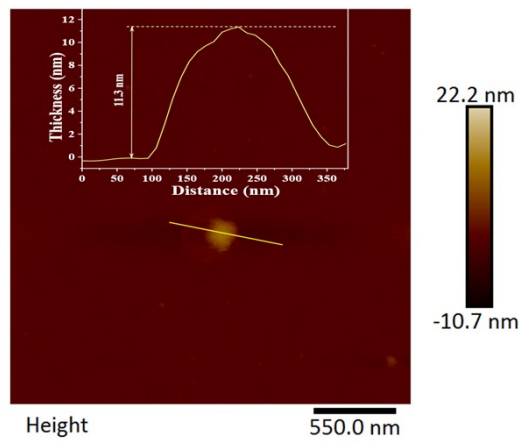


Figure S5. AFM image and the corresponding height curve (inset) of UCN.

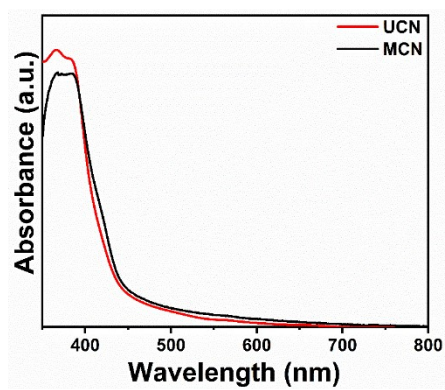
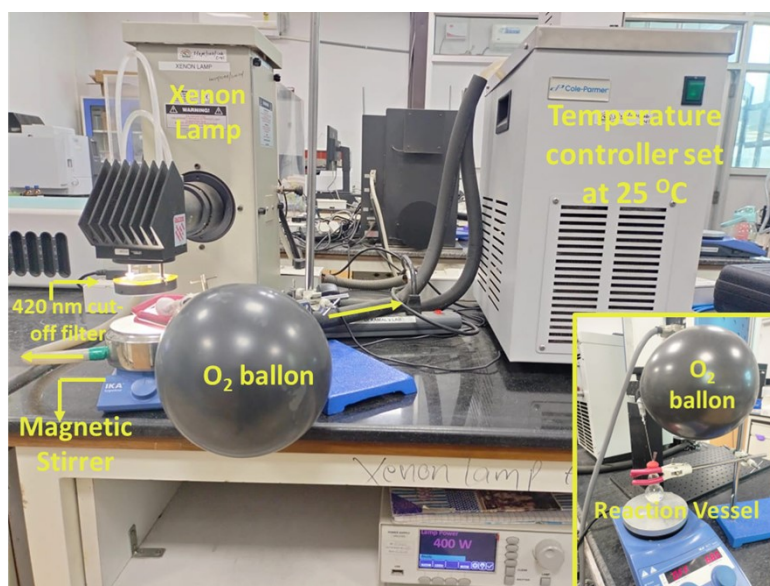


Figure S6. DR UV-Vis spectra of UCN and MCN.



Scheme S1. Photocatalytic setup for Ffal acetalization and H₂O₂ production.

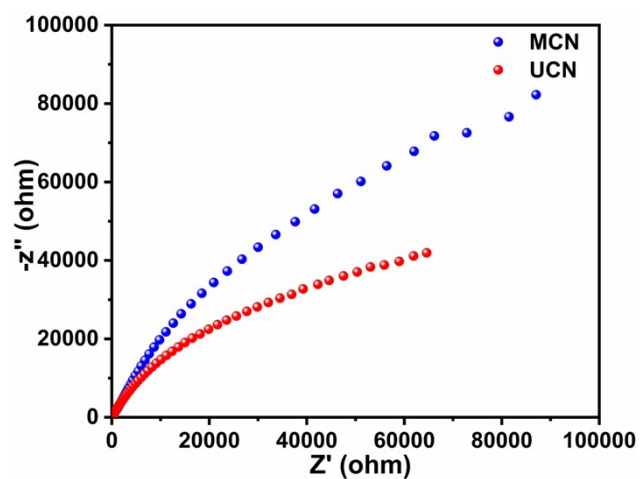


Figure S7. Nyquist plots of UCN and MCN.

The EIS-Nyquist plot could be further employed to study the charge transfer kinetics of the material. The arc radius of Nyquist plot is correlated to the charge transfer resistance (R_{ct}) at electrode/electrolyte interface. In **Figure S7**, UCN (urea-derived carbon nitride) exhibited a smaller arc radius compared to MCN (melamine-derived carbon nitride) which indicated less charge transfer resistance in UCN which eventually resulted in improved charge transfer efficiency in UCN.²

Table S1: Comparison table of Ffal acetalization with Ethylene Glycol (EG).

Entry	Catalyst	Solvent	Conditions	FD yield (%)	Fuel Yield	References
1	Kaolinitic clay	Benzene	Thermal Reflux, 2 h	93	NA	3
2	SG-[(CH ₂) ₃ SO ₃ H-HIM]HSO ₄	cyclohexane	Thermal 110 °C, 3 h	85	NA	4
3	SO ₃ H-MIL-101	cyclohexane	Thermal 80 °C, 3 h	93.1	NA	5
4	MIL-100 (Fe)	cyclohexane	Thermal 80 °C, 3 h	92.5	NA	6
5	Zr-Mont Zirconium-exchanged montmorillonite	cyclohexane	Thermal 65 °C, 2 h	89	NA	7
6	ALPO-5(1) Aluminum phosphate with Al/P ratios = 1.	1,4-dioxane	Thermal 150 °C, 24 h	95.7	NA	8
7	SAPO-34	–	Thermal 80 °C, 6 h	76.5	NA	9
8	Eosin Y (Homogeneous)	Acetonitrile	Photocatalysis Green Led, 12 h	95	NA	10
9	Phosphated-TiO ₂ (Heterogeneous)	–	Photocatalysis Air atmosphere, UV light, 16 h	56	NA	11
10	UCN	–	Photocatalysis O₂ atmosphere, visible light, 6 h	85	H₂O₂: 162 μmol g⁻¹	This work

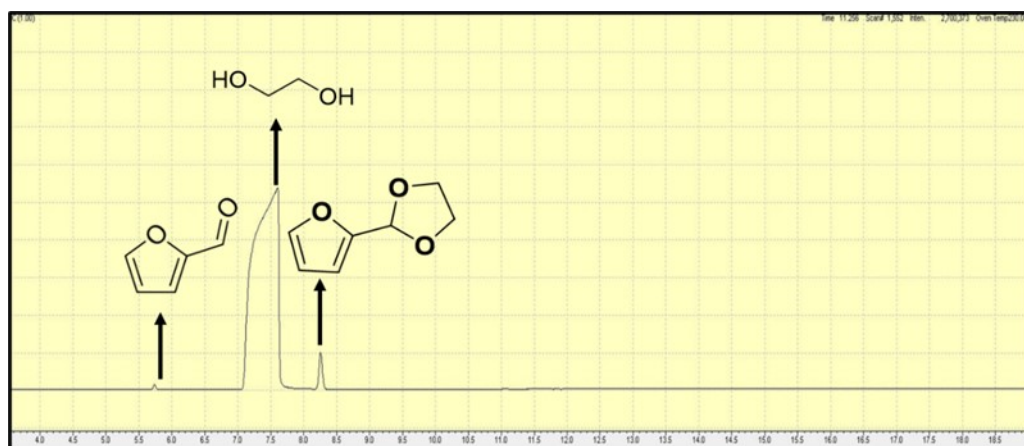


Figure S8. GC-MS-based chromatogram of reaction mixture of UCN catalyzed Ffal acetalization under O_2 environment after 6 h.

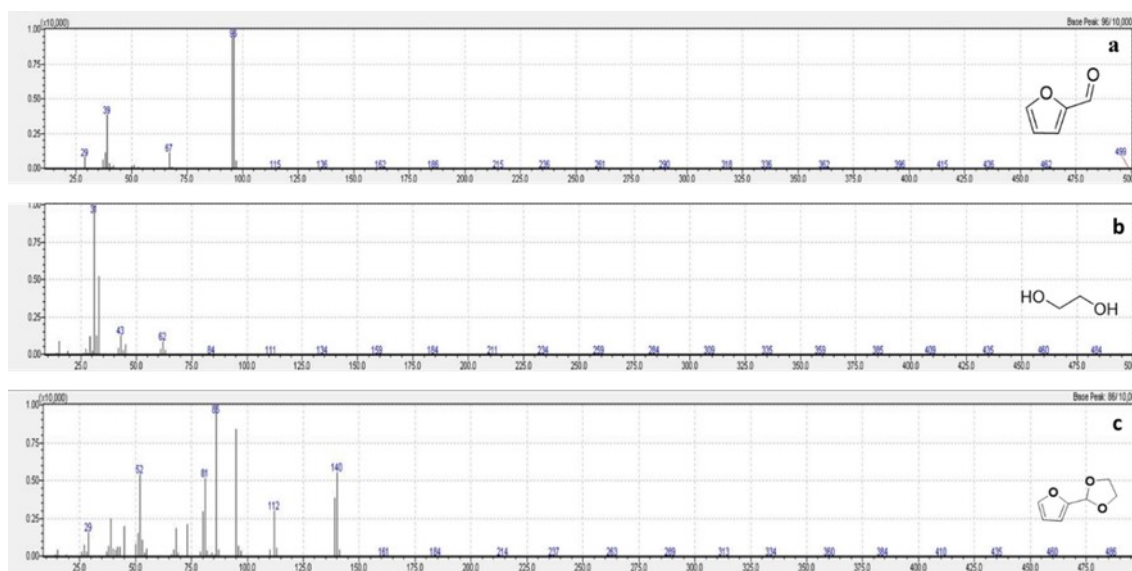


Figure S9. GC-MS graph of (a) Furfural, (b) Ethylene glycol, and (c) 2-Furyl-1,3-dioxolane.

The Ffal conversion and product selectivity were determined by the following expressions.

$$\text{Conversion (\%)} = \frac{C_o - C_t}{C_o} \times 100$$

where C_o is the reactant's initial concentration, and C_t is the reactant concentration at time t .

$$\text{Selectivity (\%)} = \frac{C_p}{C_o - C_t} \times 100$$

where C_p is the product concentration at time t , C_o is the reactant's initial concentration, and C_t is the reactant concentration at time t .

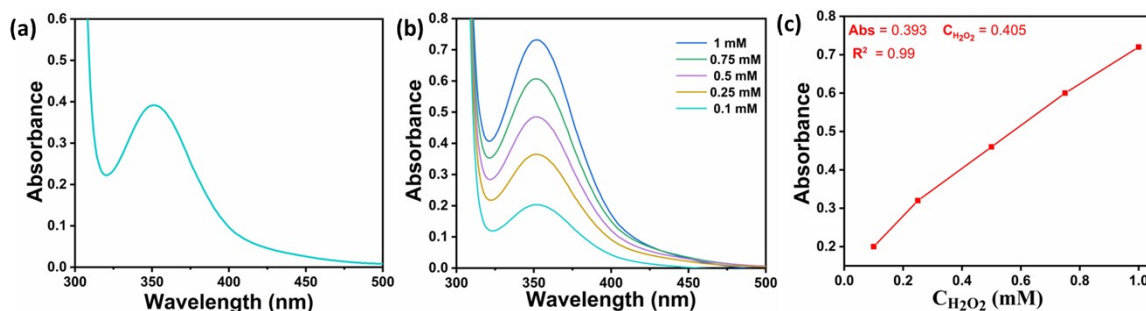
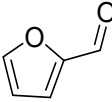
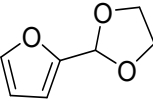
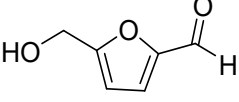
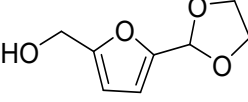
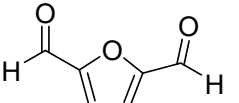
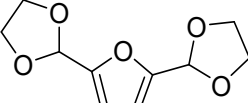
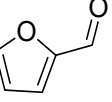
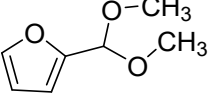
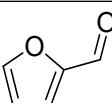
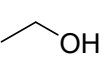
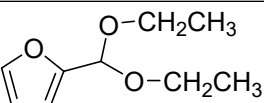


Figure S10. (a) UV-vis absorption spectra of H₂O₂ by iodometry. Reaction Conditions: Ffal (0.1 mmol), UCN (5 mg), EG (2 mL), Reaction Time (6 h), O₂ pressure (1 atm), 25 °C, and Light Source: 400 W Xenon Lamp (100 mW cm⁻²) (> 420 nm); (b) UV-vis absorption spectra of varying concentrations of H₂O₂ by iodometry; and (c) Linear fitting of standard concentration of H₂O₂.

Table S2. Substrate scope in photocatalytic acetalization of biomass-derived substrate integrated with H₂O₂ production.

Entry	Substrate	Alcohol	Acetal	Acetal yield (%)	H ₂ O ₂ (μmol/g)
1		HO-CH ₂ -CH ₂ -OH		85	162
2		HO-CH ₂ -CH ₂ -OH		73	148
3		HO-CH ₂ -CH ₂ -OH	 +	36 18	102
4		-OH		30	54
5				15	186

Reaction Conditions: Substrate (0.1 mmol), UCN (5 mg), alcohol (2 mL), reaction time (6 h), O₂ pressure (1 atm), 25 °C, and Light Source: 400 W Xenon Lamp (100 mW cm⁻²) (> 420 nm).

Table S3. Photocatalytic acetalization of Ffal under controlled conditions.

Entry	Condition	Atmosphere	FD yield (%)
1	Ideal	O ₂	85
2	TEMPO (radical scavenger)	O ₂	10
3	NH ₄ HCO ₂ (h ⁺ scavenger)	O ₂	-
4	AgNO ₃ (e ⁻ scavenger)	O ₂	87
5	Ideal	Argon	36
6	1,4-benzoquinone	O ₂	84

Reaction Conditions: Ffal (0.1 mmol), UCN (5 mg), EG (2 mL), reaction Time (6 h), O₂ pressure (1 atm), 25 °C, and Light Source: 400 W Xenon Lamp (100 mW cm⁻²) (> 420 nm).

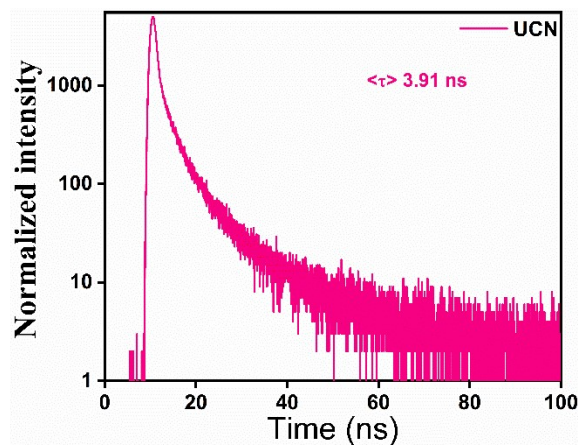


Figure S11. Time-resolved photoluminescence decay profile of UCN.

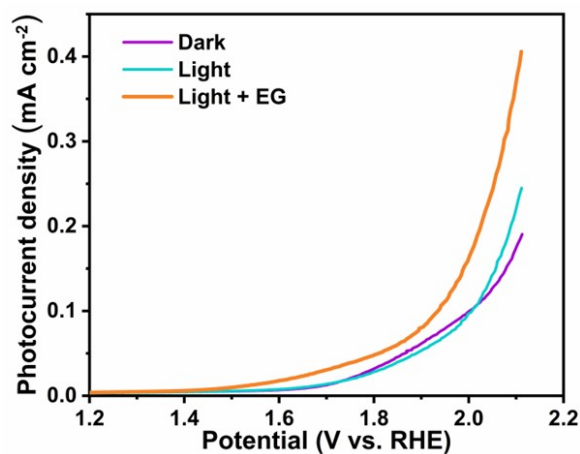


Figure S12. Photocurrent density vs potential profile of UCN in 0.2 M Na₂SO₄ under different conditions.

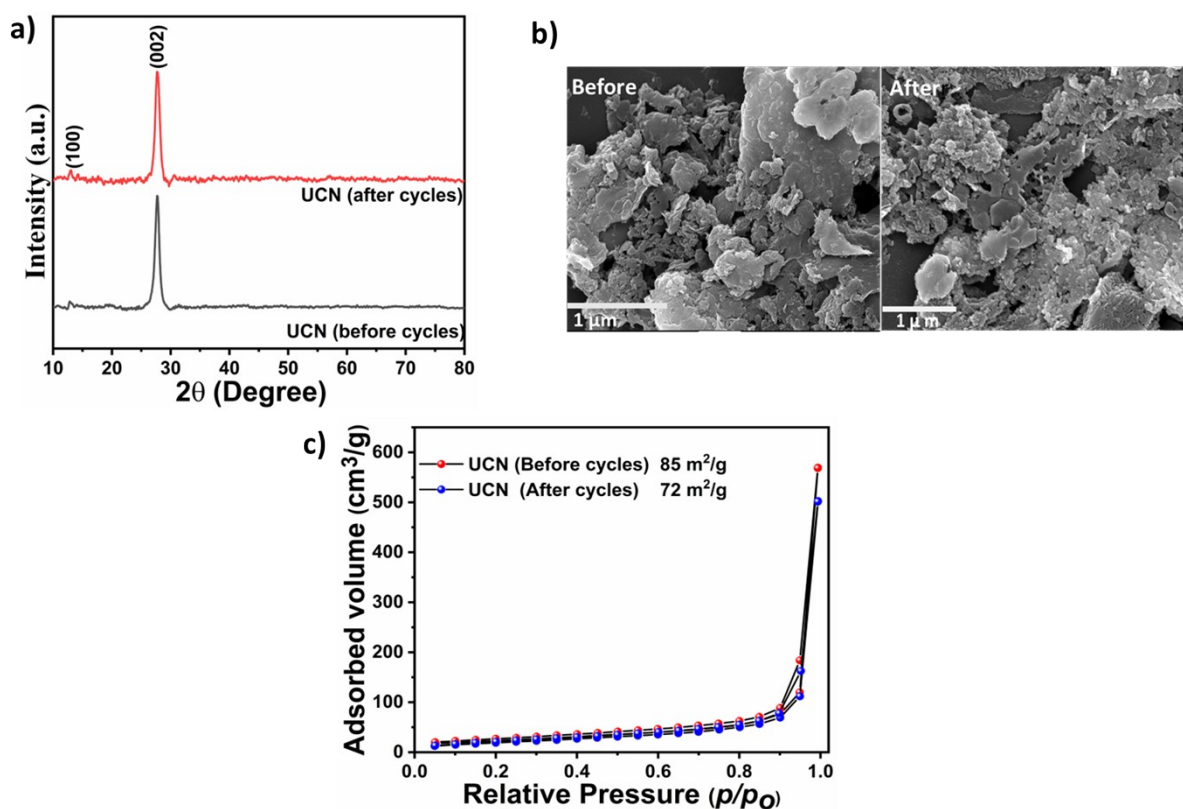


Figure S13. (a) Powder XRD patterns of UCN before and after recyclability; (b) FESEM image of UCN before and after recyclability; and (c) N₂ physisorption isotherms for UCN before and after recyclability.

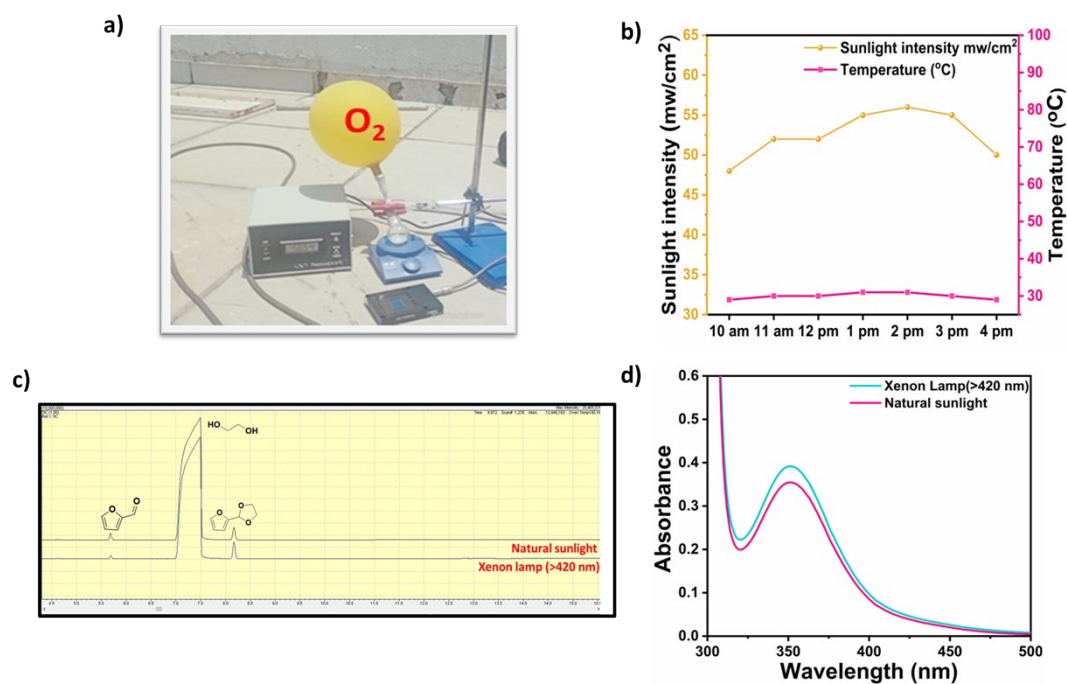


Figure S14. (a) Ffal acetalization under natural sunlight. Reaction condition: Ffal (0.1 mmol), UCN (5 mg), EG (2 mL), Reaction Time (6 h), O₂ pressure (1 atm), and Light Source: Natural sunlight; (b) Sunlight intensity and temperature profile on 4/11/2023, Sector 81, Mohali, Punjab, India; (c) GC-MS chromatogram of liquid mixture of UCN catalyzed Ffal acetalization; and (d) UV-vis absorption spectra of produced H₂O₂ through iodometry.

References:

- 1 S. Rana, K. K. Yadav, K. Sood, Ankush, S. K. Mehta and M. Jha, *Electroanalysis*, 2020, **32**, 2528–2534.
- 2 S. Q. Liu, M. R. Gao, S. Wu, R. Feng, Y. Wang, L. Cui, Y. Guo, X. Z. Fu and J. L. Luo, *Energy Environ. Sci.*, 2023, **16**, 5305–5314.
- 3 D. E. Ponde, V. H. Deshpande, V. J. Bulbule, A. Sudalai and A. S. Gajare, *J. Org. Chem.*, 1998, **63**, 1058–1063.
- 4 J. Miao, H. Wan, Y. Shao, G. Guan and B. Xu, *J. Mol. Catal. A Chem.*, 2011, **348**, 77–82.
- 5 Y. Jin, J. Shi, F. Zhang, Y. Zhong and W. Zhu, *J. Mol. Catal. A Chem.*, 2014, **383–384**, 167–171.
- 6 F. Zhang, J. Shi, Y. Jin, Y. Fu, Y. Zhong and W. Zhu, *Chem. Eng. J.*, 2015, **259**, 183–190.

- 7 A. Patil, S. Shinde, S. Kamble and C. V. Rode, *Energy and Fuels*, 2019, **33**, 7466–7472.
- 8 W. Fang and A. Riisager, *Appl. Catal. B Environ.*, 2021, **298**, 120575.
- 9 H. Song, F. Jin, Q. Liu and H. Liu, *Mol. Catal.*, 2021, **513**, 111752.
- 10 H. Yi, L. Niu, S. Wang, T. Liu, A. K. Singh and A. Lei, *Org. Lett.*, 2017, **19**, 122–125.
- 11 X. Liu, Y. Zhou, D. Zeng, H. Wang, S. Qiao, L. Zhang and W. Wang, *ChemistrySelect*, 2021, **6**, 8074–8079.